Chemical Engineering Science 314 (2025) 121791

Contents lists available at ScienceDirect

Chemical Engineering Science

journal homepage: www.elsevier.com/locate/ces

Difluoroalkylation of styrene in the continuous-flow microreactor: Process performance and Reaction kinetics

Hui Yang [a], Daofan Ma [b,*], Chunying Zhu [a], Taotao Fu [a], Guangwei Wang [b], Youguang Ma [a,*]

[a] State Key Laboratory of Chemical Engineering and Low-Carbon Technology, School of Chemical Engineering and Technology, Tianjin University, Tianjin 300072, PR China

[b] Tianjin Key Laboratory of Molecular Optoelectronic Science, Department of Chemistry, School of Science, Tianjin University, Tianjin 300072, PR China

ARTICLE INFO

Keywords:
Difluoroalkylation
Microreactor
Continuous flow
Reaction kinetics

ABSTRACT

Fluoroalkylation compounds are vital in pharmaceutical and agricultural chemistry. However, conventional batch reactor usually suffers from poor mass transfer and long reaction times. Comparatively, microreactors offer substantial improvement in mass and heat transfer for high-efficient production. Especially, it could innovate the original batch operation mode into continuous production. In this work, a highly efficient continuous flow system is constructed for styrene difluoroalkylation using CuI as a catalyst and $BrCF_2CO_2Et$ as fluorinating reagent. The influences of reactant ratios, catalyst content, alkali amount, reaction temperature and residence time on reaction performance were investigated systematically. Under optimal conditions, 80% yield was gained in only 0.5 h. The reaction time required is significantly shortened. Meanwhile, the usage of catalyst could also be reduced. Moreover, the kinetics of the styrene difluoroalkylation reaction in microreactor were studied, and the rate constant, activation energy and pre-exponential factor were obtained according to reaction kinetic model.

1. Introduction

Fluorinated compounds have a wide range of applications in pharmaceutical chemistry, pesticides, and biomaterials due to their ability to enhance the stability and bioavailability of drug molecules (Shi et al., 2022). Approximately 25 % of small molecule drugs on the pharmaceutical market contain fluorine. In the past five years, the U.S. Food and Drug Administration (FDA) has approved over 50 such drugs for treating various diseases (Wang et al., 2024).

As few organic fluorides exist naturally, thus, most fluorinated organic compounds has to rely on artificial synthesis that requires selective C-F bond construction (Britton et al., 2021). For the diverse requirements of C-F bond formation, direct fluorination and fluoroalkylation could be an effective approach (Britton et al., 2021). Direct fluorination usually requires the use of strong fluorination reagents and is carried out under high-temperature and high-pressure conditions, more importantly, its reaction selectivity is commonly low. Therefore, in this study, the fluoroalkylation method is adopted to synthesize fluorinated compound, which offers significant merits, such as higher selectivity and greater atom economy, under milder reaction conditions (Barata-Vallejo et al., 2018; Tarantino and Hammond, 2018; Zhang et al., 2020). Li et al. (Li et al., 2018a) investigated a cobalt-catalyzed reaction for synthesizing quaternary alkyl difluoride through tertiary aryl ketone difluoroalkylation. The reaction demonstrated high efficiency, broad applicability and mild conditions. Subsequently, Li et al. (Li et al., 2021) utilized a double Fe/Pd catalytic reaction to synthesize fluoroalkylated compounds, achieving good stereochemical selectivity and simplicity in operation. However, all the above fluoroalkylation reactions are usually carried out in batch reactors with low mass and heat transfer efficient. Such operational limitation compromises both reaction selectivity and conversion rate (Lee et al., 2023). In addition, the radical reaction of fluoroalkylation requires precise control of key parameters such as temperature to form specific free radical intermediates, in order to achieve efficient and selective synthesis. These problems limit the industrial application of difluoroalkylation reaction.

In recent years, flow chemistry technique has revolutionized the research and application of fluoroalkylation. This advancement is largely attributed to the use of microreactor, which has small channel diameter and high specific surface area. These characteristics enable precise control of reaction condition, thereby greatly improving mass and heat transfer performance. Meanwhile, microreactors could reduce reagent consumption, improve product quality and reaction efficiency and ensure the safety of chemical reactions (Mu et al., 2024; Russo et al., 2019; Schwolow et al., 2016). Spennacchio et al. (Spennacchio et al.,

* Corresponding authors.
E-mail addresses: daofanma@tju.edu.cn (D. Ma), ygma@tju.edu.cn (Y. Ma).

https://doi.org/10.1016/j.ces.2025.121791
Received 19 February 2025; Received in revised form 15 April 2025; Accepted 3 May 2025
Available online 5 May 2025

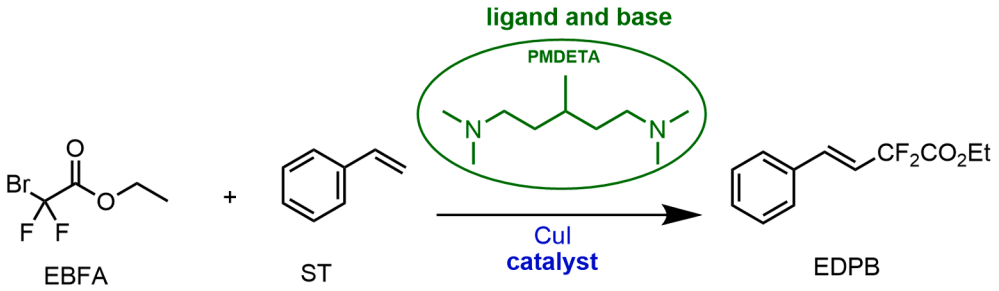

Scheme 1. Reaction for the difluoroalkylation of styrene.

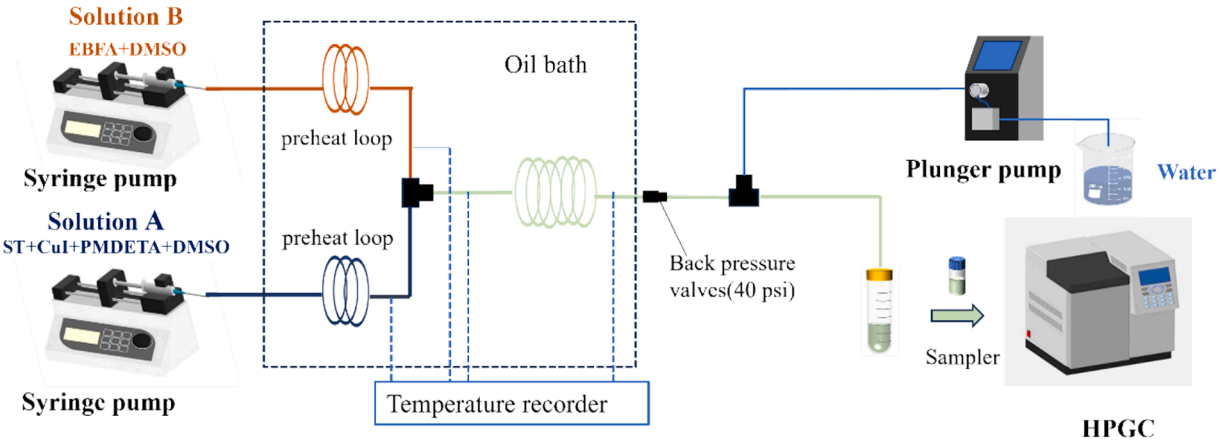

Fig. 1. Schematic diagram of the experimental set-up.

2023) developed a direct nucleophilic monofluoroalkylation strategy utilizing lithium fluorocarbene lithium in a microreactor. By precisely controlling the reaction conditions in the microreactor, the labile intermediates could be stabilized, which could effectively inhibit the occurrence of side reactions, thereby significantly improving the reaction efficiency and selectivity. Pasca et al. (Pasca et al., 2025) proposed a scalable, mild monofluoroalkylation method using visible-light-mediated photoredox catalysis in a continuous flow microreactor. This approach greatly enhances reaction efficiency and selectivity, the reaction time is reduced from 16 to 3 h, which effectively decreases light irradiation exposure and suppresses byproduct formation. Overall, this method not only optimizes the reaction conditions, but also provides a new technical path for the industrial application of fluoroalkylation reaction. In addition, microreactor could provide an ideal platform for measuring reaction intrinsic kinetics due to its high mass and heat transfer efficiency, precise mixing control, good repeatability of fluids, short cycles and extremely low reagent consumption (Li et al., 2024; Yan et al., 2022b). Compared with other fluoroalkylation methods, due to the uniqueness of the difluoromethane (CF_2) group, the precise introduction of the CF_2 group at the benzyl position could significantly improve the biological activity of the molecule, hence the aromatic difluoroalkyl compounds exhibit good biological activity. Serving as a multi-functional structural unit and a key intermediate for drug synthesis, aromatic difluoroalkyl compounds provide an efficient way for the development of new drugs (Feng et al., 2018). The determination of kinetic data for the difluoroalkylation reaction system involving aromatic compounds is of critical importance for establishing reaction kinetic model, understanding the reaction mechanism, achieving selective regulation and facilitating industrial scale-up. Nevertheless, the related study reported in the literature could be found to be still scarce.

At present, the most commonly used difluoroalkylation reagent is RCF_2X, which could be metal or photocatalyzed to the RCF_2 excited state (Dong et al., 2020), such as CF_2Br_2, HCF_2SO_2Cl, $PhCF_2Br$, $BrCF_2PO(OEt)_2$ and so on (Lemos et al., 2019). Compared with the above difluoroalkylation reagent, ethyl bromodifluoroacetate ($BrCF_2CO_2Et$, EBFA) offers broad substrate applicability, excellent functional group compatibility and high difluoroalkylation efficiency. Especially, it could provide more choices for the synthesis of complex molecules due to its high possibilities for post functionalization. Moreover, the mild reaction condition, low cost and high safety of EBFA is more applicable for commercial complicated molecular synthesis (Belhomme et al., 2015; Huang and Li, 2017; Rao et al., 2020). Among the transition metals that facilitate difluoroalkylation reactions, cuprous iodide (CuI) stands out as a cost-effective, stable and easily handled catalyst. It has been proven to be considerably effective in transferring CF_2CO_2Et groups from $BrCF_2CO_2Et$ directly to various alkenes (Wang et al., 2017). Pentamethyldiethy-lenetriamine(PMDETA) was selected as the ligand, as it could not only exhibit high catalytic activity, but also has large steric hindrance, which is conducive to the formation of stable transition metal catalyzed complex (Nanda and Matyjaszewski, 2003). In this study, a continuous flow microreactor system was constructed and utilized to investigate the difluoroalkylation reaction of styrene. The reaction employed styrene and ethyl bromodifluoroacetate as substrates and was performed in a copper–amine system (shown in Scheme 1). The influences of various process parameters, including total flow rate, residence time, reaction temperature and molar ratio on reaction were investigated systematically to determine the optimal reaction condition. Furthermore, the kinetic parameters including rate constants, pre-factor and activation energy were obtained to develop a comprehensive kinetic model and propose the possible reaction mechanism. Finally, the validation experiments were conducted to confirm the accuracy and applicability of the kinetic model.

Table 1
GC testing condition.

Device: Agilent GC-7890A	Detector: FID
Column: HP-5/30 m × 0.32 mm × 0.25 μm Carrier gas: N_2, 3 mL/min; Split ratio: 40:1 Column temperature: start at 60 °C, maintain for 3 min; 8 °C/min to 200 °C, maintain for 4 min; 30 °C/min to 320 °C, maintain for 3 min	Injection temperature: 280 °C Detection temperature: 280 °C Sample: 3 μL Quantitative method: internal standard Internal standard substance: 1, 3, 5-Trimethoxybenzene

2. Experiment

2.1. Materials

Styrene (ST, 99.5 %) was purchased from Hebei Bailingwei Hyperfine Material Co., Ltd. Ethyl bromodifluoroacetate (EBFA,99.8 %) was supplied by Shanghai Bide Pharmatech Co., Ltd. Dimethyl sulfoxide (DMSO, 99.7 %, Super dry) was obtained from Energy Chemical (Shanghai). CuI (98 %) and pentamethyldiethy-lenetriamine (PMDETA,98 %) were purchased from Heowns Biochem Technologies (Tianjin). The purities of these reagents could meet the experimental requirements, so the purification steps were not required.

2.2. Continuous flow reaction system

The microreaction system setup is shown in Fig. 1, it consists of three main units: feed unit, reaction unit and quenching unit. The two reactants ST and EBFA were fed separately. Given that EBFA could undergo transformation in alkaline conditions (Wang et al., 2017), ST, catalyst CuI and the alkaline ligand PMDETA were dissolved in DMSO and stirred by a magnetic stirring device (WM-1, INNOTEG) at room temperature to obtain solution A. EBFA was dissolved in DMSO and stirred by a magnetic stirring device (WM-1, INNOTEG) at room temperature to obtain solution B. Both solutions A and B were delivered by the syringe pumps (PHD 4400, Harvard Apparatus) under the same flow rates and preheated to reaction temperature in the 2.5 m capillary coil (PTFE, ϕ 1.587 × 1 mm). Later, the two reactive solutions were mixed in a T-type micromixer (PTFE) and then flowed into a capillary coil (PTFE, ϕ 1.587 × 1 mm) for reaction. The reaction time was controlled by using reaction coils of varying lengths. The preheating coil, the mixer and the reaction coil were immersed in an oil bath to guarantee as constant reaction temperature as possible. Under all experimental conditions, the monitoring thermocouple thermometer (YET-640, Kaipusen) showed that the inlet temperatures were the same as that of the oil bath, and the temperature changes of the outlets of the preheating loop, the micromixer, and the microreactor were less than <1.0 °C, confirming that the reaction proceeded under isothermal conditions within the microreactor. To prevent solution evaporation, a back pressure valve (40 psi) was installed at the outlet of the capillary microreactor. As the reaction is sensitive to water, pure water is chosen as the reaction quencher. Finally, after the reaction was completed at the set residence time, the deionized water solution (25 °C) was pumped into the second T-joint with a plunger pump (JJRZ-02004F, Hangzhou Jingjin Technology Co., LTD.) to quench the reaction. The quenched mixture was extracted with ethyl acetate (EA), and the organic phase products were collected and analyzed by gas chromatography (GC). In this work, all experiments were repeated 3 times and the average measured value was used as the final result.

2.3. Sample analysis

The composition of the product was quantitatively analyzed by GC using the internal standard method and 1,3,5-Trimethoxybenzene was dissolved in the reaction system as an internal standard. The organic phase, obtained after multiple extractions with EA, was analyzed through GC under the test conditions detailed in Table 1. The standard curve was established using the internal standard method by varying the ratio of each substance to the internal target. The correction factors were calculated using Eq. (1) with correlation coefficients of 0.99 for the standard curve, as illustrated in Fig. S1 of the Supplementary Material. Nuclear magnetic resonance (NMR) analysis was also conducted for verification. The GC and NMR spectra of the products are presented in Fig. S2 and Fig. S3 of the Supporting Information.

$$f_i = \frac{N_i}{N_s} \times \frac{A_s}{A_i} \tag{1}$$

where i and s are components and internal standards respectively. A and N are the integral area of the substance and the molar amount of the substance, respectively. fi is the relative correction factor for component i.

The volume flow rate of the reaction tube is calculated by Eq. (2):

$$Q_R = Q_A + Q_B \tag{2}$$

where Q_A (mL/min) is the volume flow rate of the A phase inlet tube, and Q_B (mL/min) is the volume flow rate of the B phase inlet tube.

The residence time is calculated by Eq. (3):

$$\tau = \frac{V}{Q_R} \tag{3}$$

where τ is the residence time and V is the volume of the microchannel.

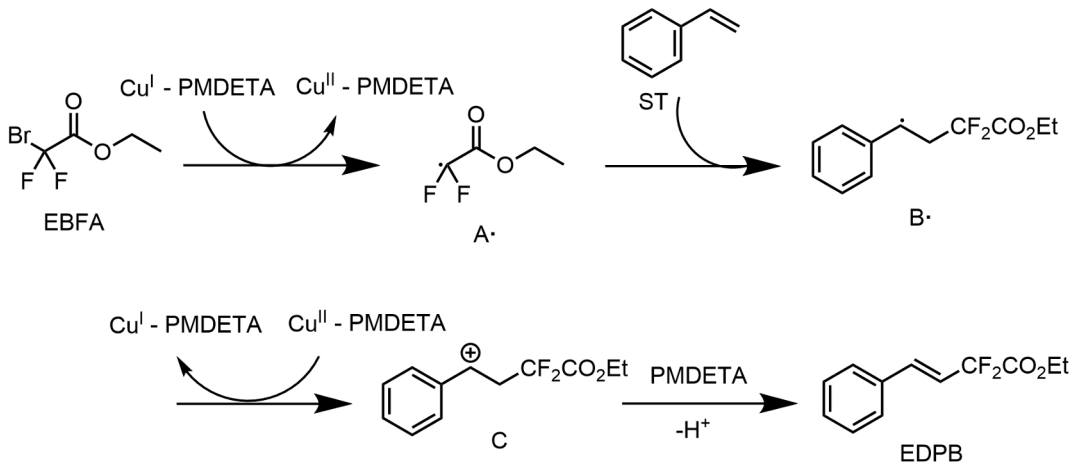

Scheme 2. The possible reaction mechanism.

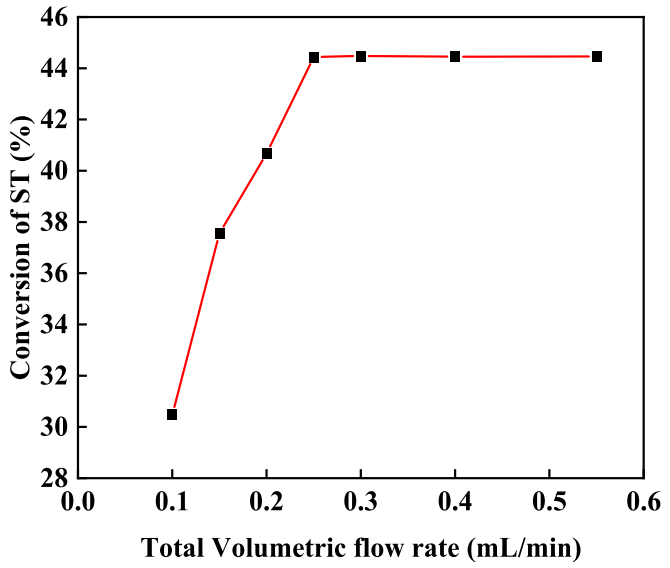

Fig. 2. Effect of total flow rate on styrene conversion. Operating condition: $C_{ST,0}$ = 0.5 mol/L,τ = 10 min, T = 80 °C, n_{EBFA}:n_{ST} = 1.5, n_{CuI}: n_{ST} = 0.1, n_{PMDETA}: n_{ST} = 1.5.

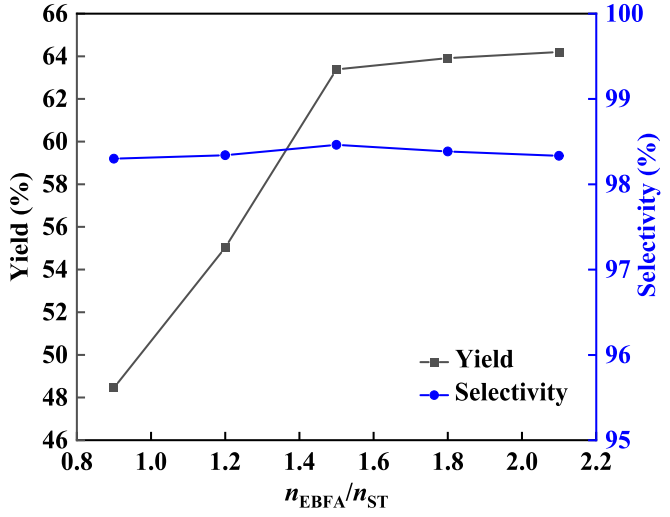

Fig. 3. Effect of molar ratio of n_{EBFA}/n_{ST} on the reaction performance. Operating condition: $C_{ST,0}$ = 0.5 mol/L, τ = 15 min, T = 85 °C, n_{CuI}: n_{ST} = 0.1, n_{PMDETA}: n_{ST} = 1.5.

The conversion of ST (x_{ST}) is a key parameter for analysis of reaction kinetics, which is calculated by Eq. (4). The yield Y of product EDPB is calculated by Eq. (5).

$$x_{ST} = 1 - \frac{f_{ST} N_s A_{ST}}{A_s C_{ST,0}} \tag{4}$$

$$Y = \frac{f_{EDPB} N_s A_{EDPB}}{A_s C_{ST,0}} \tag{5}$$

where fi is the relative correction factor of the internal standard method, A_i is the peak area detected by GC, and $C_{ST,0}$ (mol/L) is the initial concentration of styrene.

3. Results and discussion

3.1. Reaction pathway analysis

According to the literature(Afsina et al., 2021; Feng et al., 2018; Li et al., 2018b; Rao et al., 2020), the possible reaction mechanism is illustrated as Scheme 2. Initially, the EBFA is catalyzed by a catalytic complex formed from Cu(I) and the ligand, generating the 2,2-difluoroacetate radical A·. In this process, Cu(I) is oxidized to Cu(II). Subsequently, the free radical A· is added into the ST to produce a new carbon radical B· through chain transfer. Then, when radical B· undergoes electron transfer to form carbocation intermediate C, Cu(II) is reduced back to Cu(I), thereby completing the catalytic cycle. Finally, under the influence of the base PMDETA, the proton transfer occurs, generating the product EDPB. The reaction is highly stereoselective, which produces mainly *E*-isomer products.

3.2. Optimization of reaction parameters

In order to determine the optimal conditions of the difluoroalkylation reaction, a series of controlled experiments were conducted to investigate the effects of five key parameters: molar ratio of reactants (n_{EBFA}:n_{ST}), amount of catalyst (n_{CuI}:n_{ST}), amount of base (n_{PMDETA}:n_{ST}), reaction temperature (T) and residence time (τ) on the product EDPB. This method aimed to establish a correlation between these parameters and both the yield of EDPB and the conversion of ST, and to ensure the validity and scientificity of the experimental design.

3.2.1. Effect of flow rate on mixing performance

Although the difluoroalkylation reaction of styrene is homogeneous, it is less affected by interphase mass transfer resistance, inadequate mixing could still affect the reaction rate, thus effective and sufficient mixing is essential to study the intrinsic kinetics (Song et al., 2022). Due to the short molecular diffusion path in the microreactor, the fluid flow is laminar, where fluid mixing depends primarily on the channel configuration and flow velocity (Xu et al., 2023). In order to achieve the ideal mixing effect toward fully understanding of reaction kinetics and developing a more accurate reaction model, the influences of different flow velocities on the conversion of ST under the same residence time were studied, as shown in Fig. 2. It could be found that at low flow rates, the styrene conversion rate rises almost linearly with increasing flow velocity, indicating that the reaction kinetics are controlled by mass transfer. However, when the flow rate exceeds 0.25 mL/min, the styrene conversion rate would not increase further and remains nearly unchanged, implying that the reaction mixture has been sufficiently mixed. The reaction flow rate should be large enough to ensure an ideal mixture of tests under all experimental conditions. Consequently, the flow velocity of the reaction mixture was maintained at 0.3 mL/min for the subsequent experiments.

3.2.2. Effect of n_{EBFA}/n_{ST} ratio on reaction performance

To investigate the effect of the molar ratio of EBFA to ST on the reaction performance, experiments were conducted under specific conditions: the temperature of 85 °C, the time of 15 min, the molar ratio of CuI to ST is 0.1, the molar ratio of PMDETA to ST is 1.5, and the styrene concentration was fixed at 0.5 mol/L. The added amount of EBFA each time was varied. The influence of the reactant ratio on the reaction is shown in Fig. 3. The molar ratio of EBFA to ST is a critical factor in controlling the fluorination process. Lower molar ratio of EBFA to ST would lead to the reaction being insufficient, thus the styrene conversion and the product yield were also low. Nevertheless, with an excessive molar ratio of EBFA to ST, the product yield had only little change. Accordingly, an appropriate amount of EBFA is conducive to the reaction, as shown in Fig. 3. As shown in Scheme 2, the EBFA initially reacts with Cu(I) to form the 2,2-difluoroacetate radical (Feng et al., 2018) and is continuously consumed. When the molar ratio of EBFA is low, there is

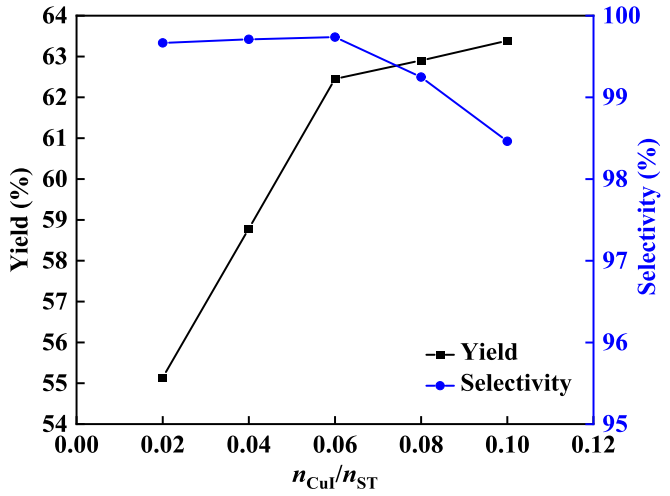

Fig. 4. Effect of molar ratio of n_{CuI}/n_{ST} on the reaction performance. Operating condition: $C_{ST,0}$=0.5 mol/L, τ=15 min, T=85℃, n_{EBFA}:n_{ST}=1.5, n_{PMDETA}: n_{ST}=1.5.

not enough EBFA to further participate in the reaction, thereby resulting in a low yield. With the increase of molar amount of EBFA, styrene is progressively transformed, accordingly leading to an increase in product yield. It was found that the optimal yield is achieved when the molar ratio of EBFA to ST reaches 1.5. Beyond this ratio, further increasing molar ratio would not significantly affect the yield, which becomes nearly leveled off, the selectivity of the reaction would also remain almost unchanged. This could be attributed to the reaction kinetics, as the maximum frequency of collisions between reactant molecules has been reached. Accordingly, the subsequent experiments were conducted with the molar ratio of EBFA to ST as 1.5.

3.2.3. *Effect of n_{CuI}/n_{ST} ratio on reaction performance*

Cu-based catalysts have been widely used in cross-dehydrogenation coupling reactions. Possible reaction mechanism is shown in Scheme 2, EBFA firstly forms the 2,2-difluoroacetate radical through the action of Cu(I), which is oxidized to Cu(II) and stabilized by the PMDETA complex in the system(Afsina et al., 2021), and then Cu^{II} −PMDETA reacts with the intermediate through the single electron transfer process to form Cu^{I}−PMDETA(Rao et al., 2020). Through its own REDOX, the reaction is advanced by a catalytic cycle formed through two single-electron transfers. As the amount of CuI in the catalyst could affect the generation of the 2,2-difluoroacetate radical and the concentration of free radical intermediates in the reaction process, thus the reaction rate would also be affected. As shown in Fig. 4, the yield of product EDPB increases rapidly in initial stage with the rise of the molar ratio of CuI, and then the increase would become slowed down. Meanwhile, the selectivity begins to decline. This trend could be attributed to that the growth of the concentration of the 2,2-difluoroacetate radical leads to more fluoroalkyl radicals reacting with styrene. In this case, the amount of styrene involved in the reaction per unit time would increase, which results in higher conversion rate of styrene and corresponding increase in product yield. However, when the molar ratio of CuI to styrene reaches 0.06, the increasing rate of product yield slows down, suggesting that the effect of the increase of catalyst amount on the reaction becomes insensitive beyond this point. The further increase of CuI would lead to an overconcentration of catalyst in the reaction system, and the interaction between catalyst molecules may appear and destroy the single electron transfer process, as the stereoselectivity of the reaction is mainly dominated by the electron transfer path in the process (Ghattas et al., 2006). As shown in Fig. 4, with the increase of CuI concentration, the catalyst aggregation effect would be significantly enhanced, which could not only affect the spatial orientation of electron transfer process, but also destroy the stability of free radical intermediates. Moreover, excessive catalyst concentration would change the activation energy barrier, leading to a deviation from the preferred chemical pathway, hence decreasing the selectivity of the target product. Therefore, subsequent experiments were conducted with the molar ratio of CuI to styrene as 0.06.

3.2.4. *Effect of n_{PMDETA}/n_{ST} ratio on reaction performance*

PMDETA plays an important role in the catalyst cycle, the reaction could not occur in the absence of ligands, and the choice of ligands determines the chemical process of the reaction (Jia et al., 2018). As shown in Scheme. 2, PMDETA serves a dual role as both a ligand and a base, forming a highly reactive catalyst complex with Cu. This complex stabilizes intermediates and facilitates the subsequent deprotonation process(Feng et al., 2015; Taylor et al., 2010). Fig. 5 depicts the effect of the molar ratio of PMDETA to ST on the substrate consumption and the product yield in the capillary microreactor. As shown in Fig. 5(a), the reaction selectivity remains relatively stable at over 99 %. When the molar ratio of PMDETA to ST is increased from 0.9 to 1.5, the yield of the product EDPB increases significantly. The enhancement could be attributed to the deprotonation reaction involving PMDETA, which

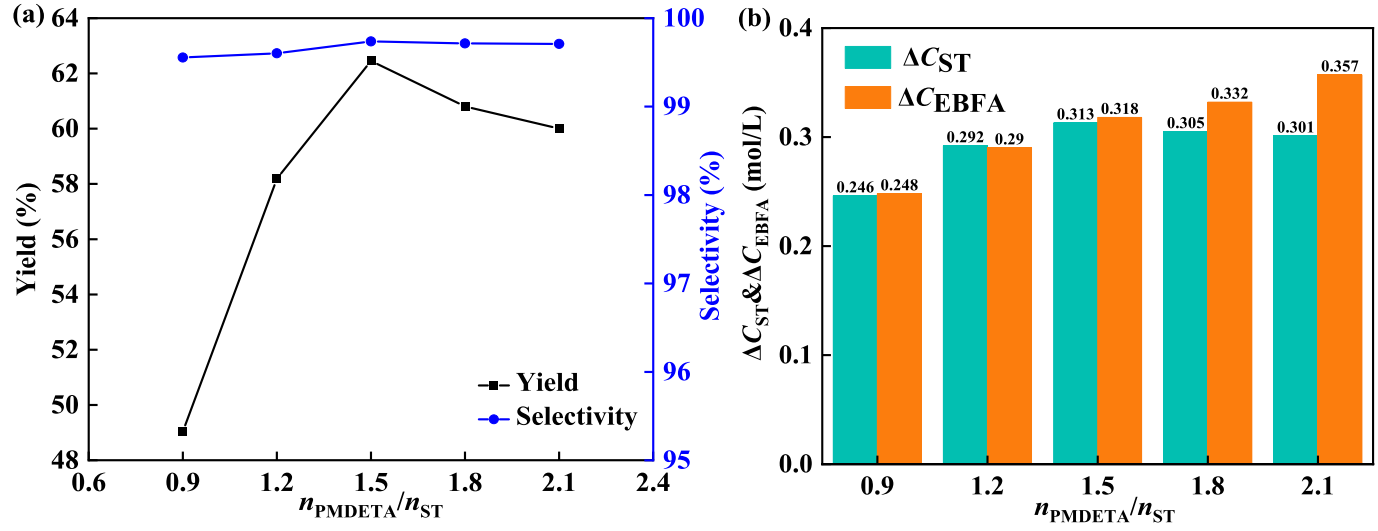

Fig. 5. Effect of molar ratio of n_{PMDETA}/n_{ST} on the reaction performance. (a) Variation of yield and selectivity of EDPB. (b) Consumption of ST and EBFA. Operating conditions: $C_{ST,0}$ = 0.5 mol/L, τ = 15 min, T=85 °C, n_{EBFA}:n_{ST} = 1.5, n_{CuI}: n_{ST} = 0.06.

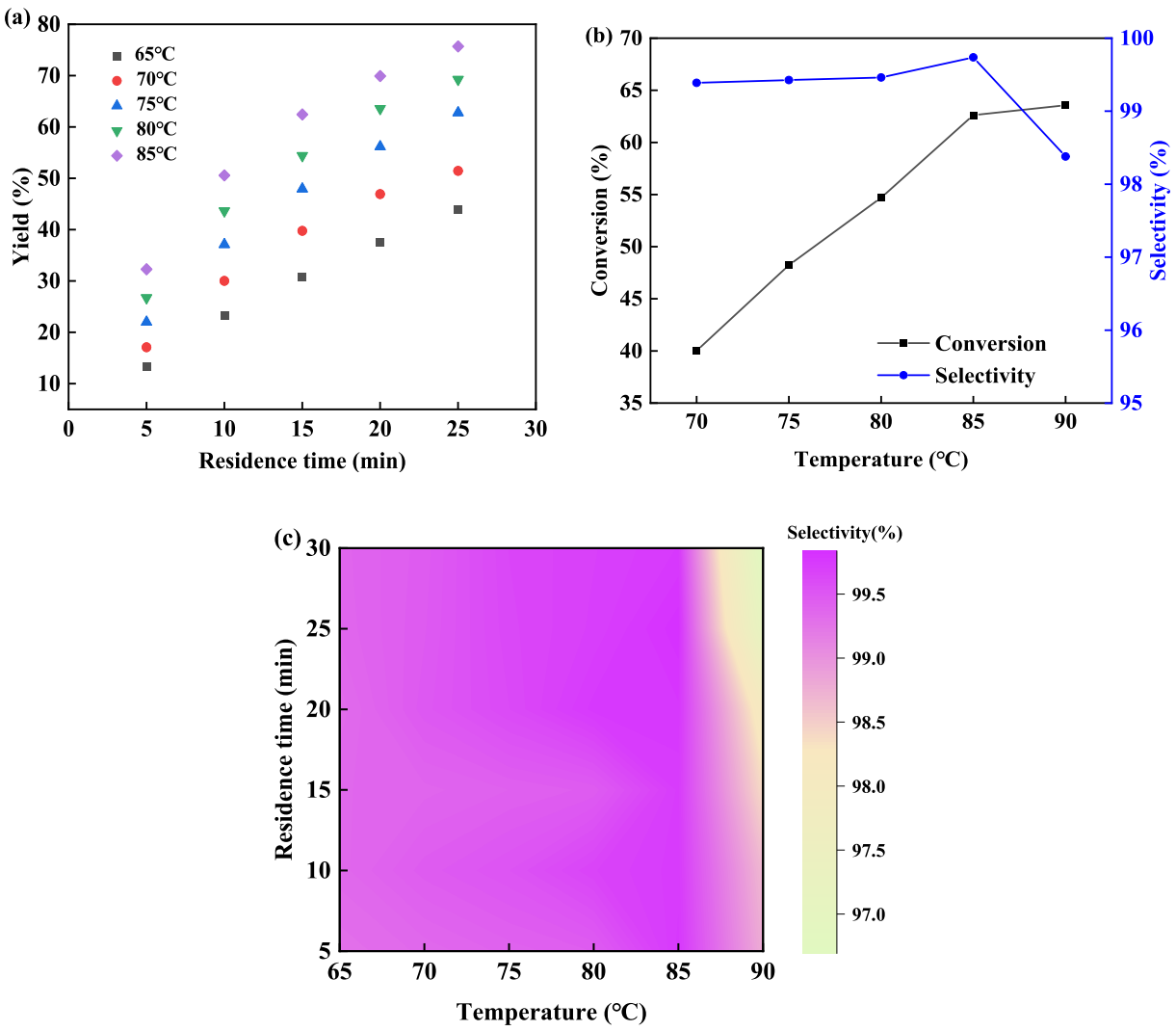

Fig. 6. Effects of temperature and residence time on reaction performance. (a)The yields of EDPB at different temperatures and residence times. (b). Effect of temperature on the reaction. ($\tau = 15$ min). (c). Effect of temperature and residence time on the selectivity of EDPB. Operating conditions: $C_{ST,0} = 0.5$ mol/L, n_{EBFA}:$n_{ST} = 1.5$, n_{CuI}: $n_{ST} = 0.06$, n_{PMDETA}: $n_{ST} = 1.5$.

Table 2
The measured process parameters are compared to the literature values.

Reactor types	Solvent	Fluoroalkyla-tion agents	n_{1a}/n_{2a}	Catalyst (mol%)	T (°C)	Time(h)	Yield (%)	Inert Gas usage
Batch (Lai et al., 2017)	DMSO	ICF_2CO_2Et	2:1	[Cu] (5 %)	60	46	45	Yes
Batch(Wang et al., 2017)	DMSO	$BrCF_2CO_2Et$	1:1.5	[Cu] (10 %)	80	12	77	Yes
Batch (Zhang et al., 2015)	1,4-Dioxane	$BrCF_2CO_2Et$	2:1	[Pd] (10 %)	80	24	65	No
Batch (this work)	DMSO	$BrCF_2CO_2Et$	1:1.5	[Cu] (6 %)	85	12	34	No
Microreactor (this work, optimal)	DMSO	$BrCF_2CO_2Et$	1:1.5	[Cu] (6 %)	85	0.5	80	No

Note: 1a is an alkene and 2a is a fluoroalkylation agent.

directly affects the formation of EDPB. The increase of PMDETA concentration would lead to higher reaction rate. However, when the molar ratio exceeds 1.5, further addition of PMDETA would cause a decline in EDPB yield. This may be stemming from the excessive concentration of PMDETA, which potentially increases its interaction with EBFA, accordingly resulting in the formation of by-products. As a nucleophile, PMDETA could attack the carbon atom that is combining with the bromine substituent in EBFA, thereby promoting the separation of bromine and finally generating ethyl 2-(dimethylamino)-2-oxoacetate (Wang et al., 2017). In this experiment, as the GC is difficult to accurately measure the EBFA concentration, NMR was employed to detect the consumption of EBFA under varying ligand concentration. It could be approximately calculated from the NMR detection results that the consumption of EBFA was significantly higher than that of ST when the molar ratio of PMDETA to ST was greater than 1.5 (as shown in Fig. 5 (b)). Consequently, it could be concluded that when concentration of PMDETA is excessively high, the overconsumption of EBFA contributes to the downward trend of yield. Therefore, subsequent experiments were conducted with the PMDETA to ST molar ratio of 1.5.

3.2.5. *Effects of temperature and residence time on reaction performance*

The conversion and product selectivity are sensitive to reaction temperature and residence time, thus the influences of temperature and residence time on reaction performance are investigated, as shown in

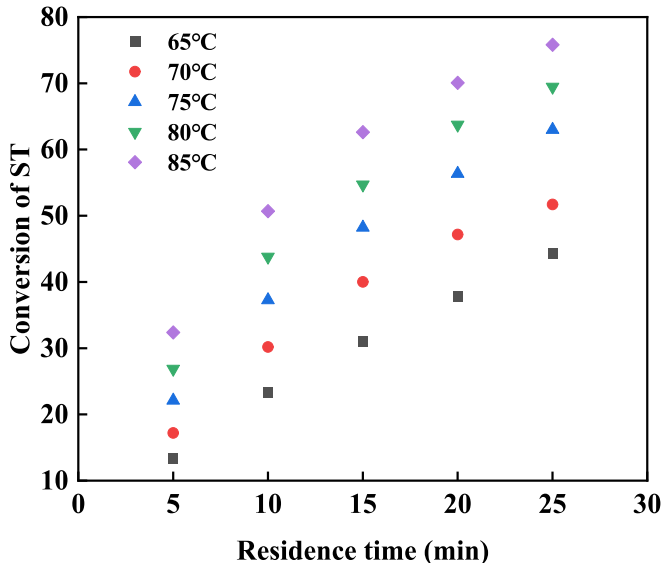

Fig. 7. The conversion of ST at different temperatures and residence times. Operating conditions: $C_{ST,0}$ = 0.5 mol/L, n_{EBFA}:n_{ST} = 1.5, n_{CuI}: n_{ST} = 0.06, n_{PMDETA}: n_{ST} = 1.5.

Fig. 6. At given temperature, the yield of the product increases with the extension of the residence time. The reaction process relies on the REDOX cycle of the catalyst itself (Lai et al., 2017). With the extension of reaction time, the ST conversion amount gradually increases, hence leading to a corresponding rise in product yield (Fig. 6a). As shown in Fig. 6b, the ST conversion rate increases with temperature at a constant residence time. The initiation process of free radicals needs a proper temperature. In the case of lower temperatures, the activity of the initiator remains also lower, thus, initiation process is prolonged. When the temperature rises, the activity of initiator increases and the initiation time becomes shortened, which facilitates the generation of the 2,2-difluoroacetate radical. According to the Arrhenius equation, the reaction rate increases with temperature. In the initial stage, as the temperature gradually rises to 85 °C, the conversion rate of ST increases significantly. However, once beyond this temperature, the variation of ST conversion slows down. At lower temperature, the reaction rate is slower due to the lower energy of the reaction system, which inhibits the occurrence of side reactions and facilitates the conversion of reactants to target products. With the increase of temperature, the reaction rate increases correspondingly, and the number of the 2,2-difluoroacetate radical formed by Cu-catalyzed transformation of EBFA per unit time would increase, hence the conversion rate rises. Conversely, at higher temperature, the energy of the reaction system becomes sufficient, the reaction would become possible to overcome high energy barriers to generate by-products (Chen et al., 2024). As the temperature exceeds 85 °C, the increased molecular motion induces competing reaction pathways, accordingly bringing about a significant increase in the reaction complexity. This complexity leads to the formation of multiple side-products, thereby reducing the selectivity of the reaction. Consequently, the selectivity of EDPB decreases at elevated temperature. Therefore, to avoid the generation of by-products, appropriate residence time and reaction temperature are adopted to obtain accurate kinetic data and model. Due to the short residence time and low reaction temperature, the selectivity of the main product is more than 99 %, and the by-products formed are slight even negligible. The relationship between reaction selectivity, reaction temperature, and residence time is illustrated in Fig. 6(c). When the reaction temperature is below 85 °C and the residence time ranges from 5 to 25 min, high reaction selectivity could be always attained.

Comprehensively, the optimal reaction conditions were identified as follows: a molar ratio of EBFA to ST is 1.5, a molar ratio of PMDETA to ST is 1.5, and a molar ratio of CuI to ST is 0.06. Based on these optimized conditions, kinetics test experiments were subsequently conducted.

3.3. Comparison of the difluoroalkylation reaction in the microreactor and the batch reactor

Furthermore, a conventional batch reaction was utilized to perform comparative experiment to assess the performance of the microreactor used. Each substance with a concentration corresponding to the optimal reaction conditions of the microreactor (n_{EBFA}: n_{ST} = 1.5, n_{CuI}: n_{ST} = 0.06, n_{PMDETA}: n_{ST} = 1.5) was respectively added to the reaction tube and dissolved in DMSO, with total amount of 2 mL. The reaction mixture was then subjected to a constant temperature of 85 °C and stirred continuously for 12 h, without the use of an inert gas atmosphere. The yield of EDPB was determined by GC.

Table 3
Values of k at different temperatures.

Temperature(°C)	65	70	75	80	85
k (L mol^{-1} s^{-1})	0.00063	0.00085	0.00120	0.00152	0.00193

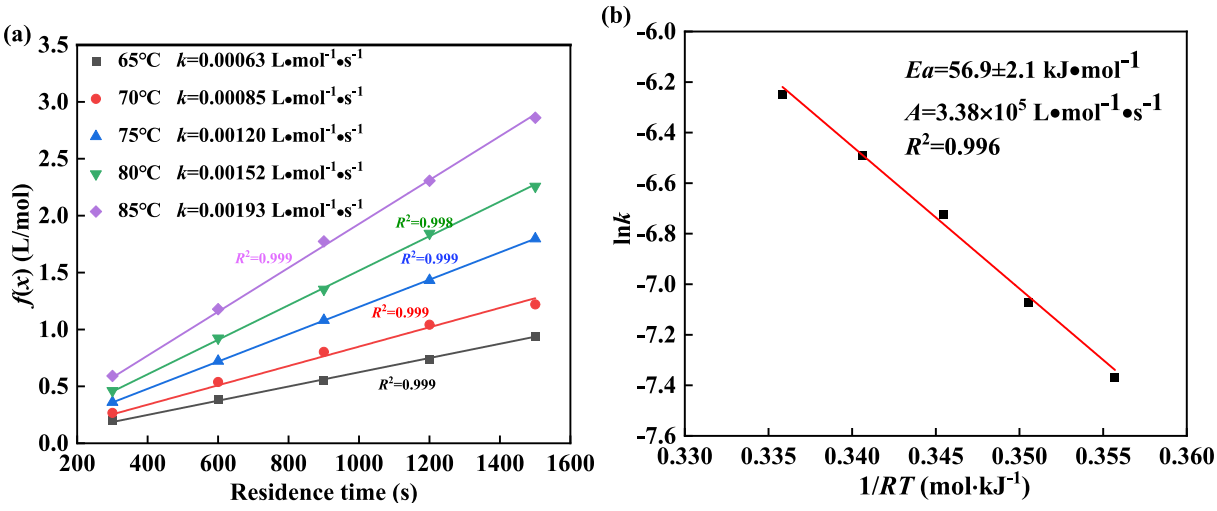

Fig. 8. Determination of kinetic parameters. (a) Plot of $f(x)$ versus residence time at temperature range of 65-85 °C. (b) Plot of ln$k$ versus $1/RT$. Operating conditions: $C_{ST,0}$ = 0.5 mol/L, n_{EBFA}:n_{ST} = 1.5, n_{CuI}:n_{ST} = 0.06, n_{PMDETA}: n_{ST} = 1.5.

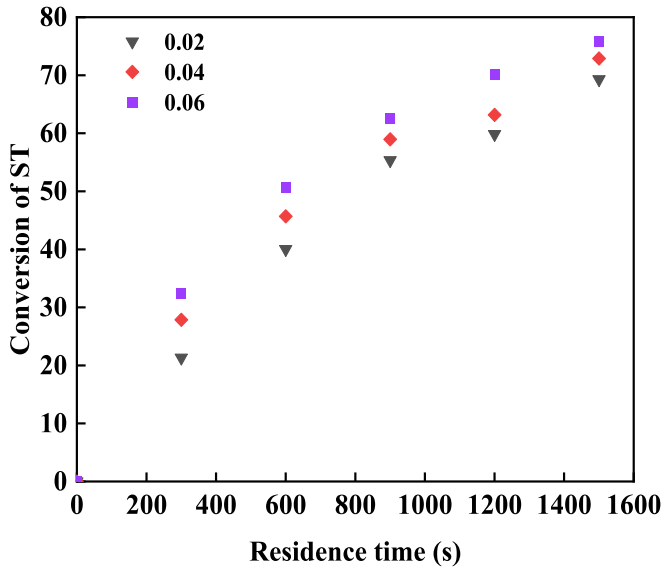

Fig. 9. The conversion of ST at different molar ratio of CuI and residence times. Operating conditions: $C_{ST,0}$ = 0.5 mol/L, T = 85 °C, n_{EBFA}:n_{ST} = 1.5, n_{PMDETA}: n_{ST} = 1.5.

In addition, the yield of difluoroalkylation of styrene was also compared with the results of similar reactions in batch reactors reported in the literature, as shown in Table 2. Lai et al.(Lai et al., 2017) use a batch reactor and conduct a reaction under N_2 protection at 60 °C for 46 h, and the target product was obtained only with a 45 % yield. Similarly, under an argon atmosphere, Wang et al.(Wang et al., 2017) conducted the reaction at 80 °C for 12 h, affording a 77 % yield. On the contrary, in the absence of inert gas protection, the desired product was observed with a yield of 65 % after 24 h at 80 °C condition in the study of Zhang et al(Zhang et al., 2015). In this experiment, the yield after 12 h in the reaction tube at 85 °C was only 34 %. Compared to batch reactor, microreactor offers the advantages of closed systems and internal stability, making them less susceptible to intrusion by media such as water and air. This effectively eliminates the impact of oxygen on free radical reactions. Therefore, the reaction in microreactor has no requirement for inert gas protection, which reduces catalyst usage and shortens residence time. Remarkably, microreactor achieves an 80 % product yield and meanwhile offers notable advantage in product quality. Because the microreactors, utilizing continuous flow operations, effectively prevent the common issue of uneven concentration distribution found in batch reactors, thereby significantly enhancing reaction uniformity. Moreover, the short molecular diffusion distance and rapid mixing, along with excellent plug flow characteristics and efficient heat transfer, create an ideal environment for homogeneous reactions, showing significant advantages over batch reactors. Overall, the continuous flow reaction technique significantly simplifies the operation, reduces the use of inert gases and catalysts, and alleviates operational complexity, accordingly offering a more efficient and cost-effective solution for industrial applications.

3.4. Kinetic research of difluoroalkylation in microreactors

The understanding of reaction kinetics is an important foundation for industrial application. Although transition metal-catalyzed difluoroalkylation reactions have been paid considerable attention, the kinetic study of these reactions remains still insufficient. The reaction rate equations could be derived as follows (Pintauer and Matyjaszewski, 2008):

Initiation:

$$EBFA + Cu^{I}\text{ - }PMDETA \underset{k_{deact1}}{\overset{k_{act1}}{\rightleftharpoons}} A\cdot + Cu^{II}\text{ - }PMDETA \quad (6)$$

Propagation:

$$A\cdot + ST \xrightarrow{k_p} B\cdot \quad (7)$$

Termination:

$$B\cdot + Cu^{II}\text{ - }PMDETA \xrightarrow[PMDETA]{kt} EDPB + Cu^{I}\text{ - }PMDETA \quad (8)$$

According to the reaction mechanism, the expression of equilibrium constant (K_A) is obtianed in Eq. (9)(Matyjaszewski and Tsarevsky, 2014).

$$K_A = \frac{k_{act1}}{k_{deact1}} = \frac{[A\cdot]\left[Cu^{II}\text{ - }PMDETA\right]}{[EBFA]\left[Cu^{I}\text{ - }PMDETA\right]} \quad (9)$$

where k_{act1} is the activation rate constant and k_{deact1} is the deactivation rate constant. [A·], [Cu^{I}-PMDETA], [Cu^{II}-PMDETA] and [EBFA] is the concentration of free radical A·, Cu(I) complex, Cu(II) complex and EBFA, respectively.

Moreover, DFT calculation of a similar difluoroalkylation was explored by Laru et al. (Laru et al., 2024) based on the analysis of the free energy change and free energy barrier of the reaction. The result indicated that the free energy barrier for the difluoro radical addition

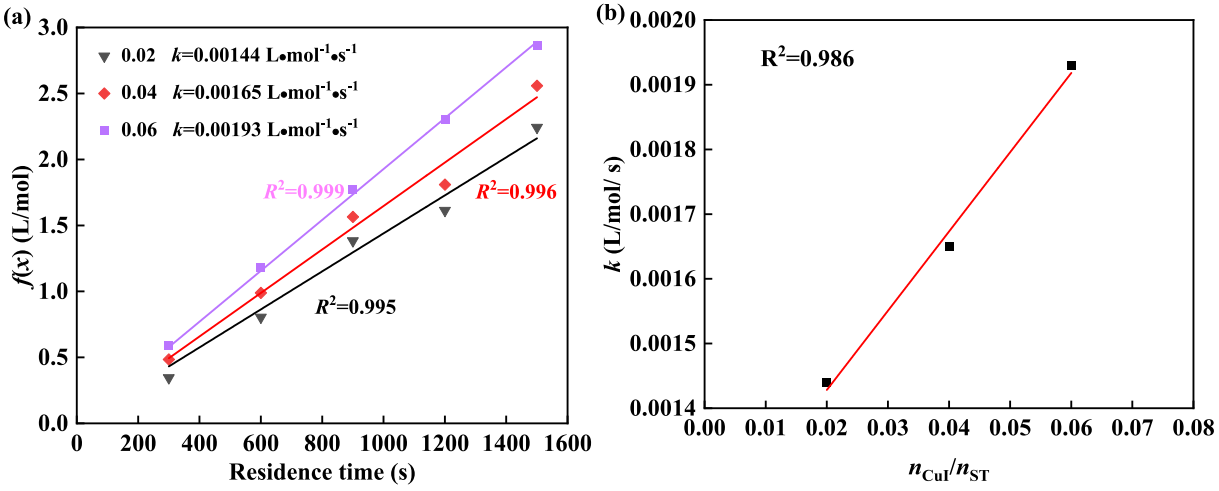

Fig. 10. Determination of kinetic parameters. (a) Plot of $f(x)$ versus residence time at molar ratio of CuI at 0.02–0.06. (b) Plot of k versus n_{CuI}:n_{ST}. Operating conditions: $C_{ST,0}$ = 0.5 mol/L, T = 85 °C, n_{EBFA}:n_{ST} = 1.5, n_{PMDETA}: n_{ST} = 1.5.

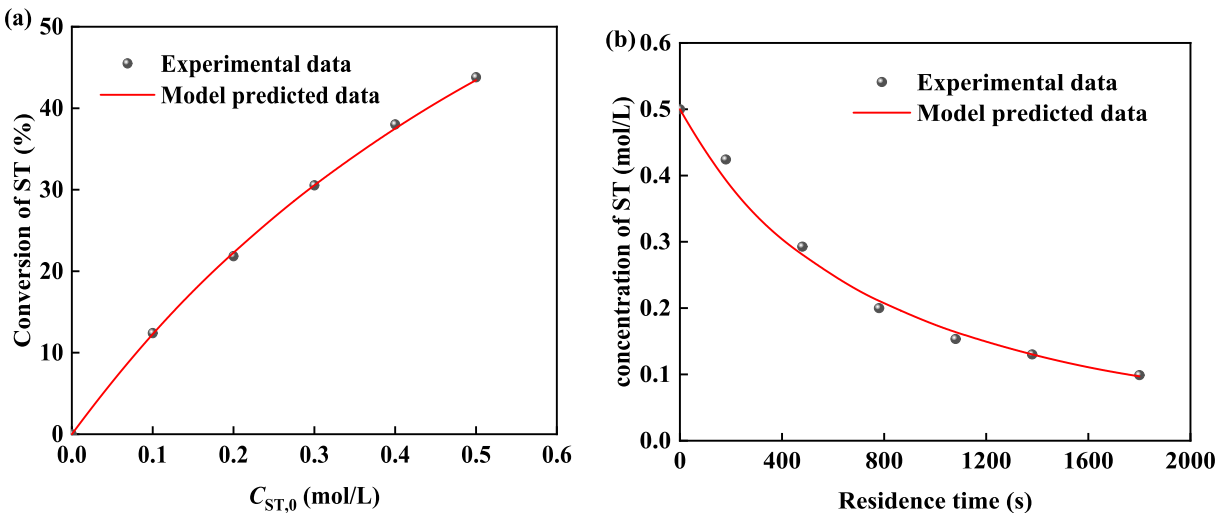

Fig. 11. Kinetic model validation. Lines represent model-predicted data, dots are experimental data. (a). The experimental and predicted results for the conversion of ST versus the initial concentration. (T = 80 °C, τ = 10 min); (b). The experimental and predicted results for the concentration of ST versus the residence time. (T = 85 °C). Operating conditions: n_{EBFA}:n_{ST} = 1.5, n_{CuI}: n_{ST} = 0.06, n_{PMDETA}: n_{ST} = 1.5.

step is higher than that for any subsequent steps, implying that the formation of the C-C bond is the rate-determining step of the overall reaction. Besides, the transition metal-catalyzed radical initiation mechanism is also consistent with the reaction pathway reported by Wu et al. (Wu et al., 2019), which is faster than the radical addition process. Therefore, the process of free radical A· reacting with ST to form carbon free radical B· is the rate-determining step of the reaction.

$$r = -\frac{dC_{ST}}{d\tau} = k_p[A\cdot][ST] \tag{10}$$

where k_p is the radical addition rate reaction constant. τ is the residence time of the reactants. [ST] is the concentration of ST.

The expression of the concentration of free radical A· could be obtained by transforming Eq. (9).

$$[A\cdot] = K_A\frac{[Cu^I\text{ - }PMDETA][EBFA]}{[Cu^{II}\text{ - }PMDETA]} \tag{11}$$

Substituting Eq. (11) into Eq. (10):

$$r = -\frac{dC_{ST}}{d\tau} = k_pK_A\frac{[Cu^I\text{ - }PMDETA][ST][EBFA]}{[Cu^{II}\text{ - }PMDETA]} \tag{12}$$

The catalyst complexes maintain a dynamic equilibrium in the reaction process, so the ratio of their concentration could be considered as a constant (Krys and Matyjaszewski, 2017). Hence, Eq. (12) could be converted into Eq. (13).

$$r = -\frac{dC_{ST}}{d\tau} = k[ST][EBFA] \tag{13}$$

where k is the reaction rate constant.

Due to the low volatility and issues with thermal stability of EBFA, it is not readily to produce peaks on GC, thus EBFA concentration could not be accurately detected. It can be obtained from Eq. (13), the overall reaction order for the styrene difluoroalkylation process is determined to be 2, and the concentration of EBFA could be calculated according to the conversion of ST and mass balance (14). Substituting Eq. (14) to Eq. (13) and integrating the equation, the relation between the conversion of ST and residence time could be deduced as given by Eq. (15), where η = $[EBFA]_0/[ST]_0$ is the ratio of the initial concentration of EBFA and ST (Yan et al., 2022a). Substituting the initial conditions τ = 0 and x_{ST} = 0 into Eq. (15), it could be obtained that $C = \ln\eta$. Consequently, Eq. (15) could be rewritten as Eq. (16).

$$[EBFA] = [EBFA]_0 - ([ST]_0 - [ST]) \tag{14}$$

$$\ln\left(\frac{\eta - x_{ST}}{1 - x_{ST}}\right) = (\eta - 1)[ST]_0k\tau + C(\eta \neq 1) \tag{15}$$

$$f(x) = \frac{\ln\frac{\eta - x_{ST}}{(1-x_{ST})\eta}}{(\eta - 1)[ST]_0} = k\tau(\eta \neq 1) \tag{16}$$

To obtain accurate kinetic results, the conversion rates of ST were measured at various temperatures and residence times in the microreactor, as shown in Fig. 7. By substituting the conversion data into Eq. (16), the relationship between $f(x)$ and τ at different temperatures could be obtained, as shown in Fig. 8(a). The slope (k) of the curve is the value of the reaction rate constant k at different reaction temperatures, and the value of k is summarized in Table 3. Fig. 8(b) shows the relationship curve between ln$k$ and $1/RT$.

According to Arrhenius Eq. (17):

$$\ln k = \ln A - \frac{E_a}{RT} \tag{17}$$

The activation energy (Ea) and pre-exponential factor (A) are obtained, which are 56.9 ± 2.1 kJ·mol^{-1} and 3.38 × 10^{5}L·mol^{-1}·s^{-1}, respectively.

To explore the effect of catalyst concentration on kinetics, the evolution of ST conversion against CuI concentration and residence time were measured under the given reaction temperature, as shown in Fig. 9. By substituting the conversion rate data into Eq. (16), the relationship between $f(x)$ and τ under different CuI molar ratios could be obtained, as shown in Fig. 10(a). The values of rate constant k at different CuI concentrations could be calculated by the curve slope, it could be easily seen from Fig. 10(b) that the reaction rate constant increases almost linearly with the molar ratio of the catalyst.

3.5. Kinetic model validation

To verify the kinetic model, a series of experiments were performed at various initial concentrations of ST. The conversion rate of ST was used to compare the deviation between the experimental data (x_e) and the predicted results (x_m). The accuracy of the kinetic equation is assessed by the mean relative error δ, which is determined by the following calculation:

$$\delta = \frac{|x_e - x_m|}{x_m} \times 100\% \quad (18)$$

As shown in Fig. 11(a), the predicted conversion rate is in good agreement with the experimental data ($\delta \leq 2.0$ %), indicating the reliability of the kinetic model and the accuracy of the extensive experimental data obtained from the microreactor. As is well known, the reaction kinetic model is critically important for tailoring a desirable reactor, as it could predict the concentration change of ST at different residence times. It could be clearly found from Fig. 11(b) that the model prediction values match experimental data well, indicating the excellent predicting performance of the present model.

4. Conclusion

In this work, a continuous flow microfluidic system was successfully designed and constructed to investigate the kinetics of styrene difluoroalkylation. The influences of total flow rate, molar ratios of EBFA, CuI, and PMDETA to ST, temperature, and residence time on the reaction performance were studied and the optimal conditions were determined: molar ratio of EBFA to ST of 1.5, PMDETA to ST of 1.5, and CuI to ST of 0.06, the temperature 85 °C. Compared to batch reactors, the microchannel reactor significantly reduced reaction time, simplified reaction steps, and greatly enhanced synthesis efficiency, achieving an 80 % yield within 30 min. Additionally, a kinetic model was developed based on the free radical mechanism, and a series of kinetic parameters were obtained. The reaction rate constant was found to increase linearly with the catalyst concentration and the reaction rate constants at various temperatures are determined, with the activation energy of 56.9 ± 2.1 kJ·mol^{-1} and the pre-exponential factor of 3.38 × 10^{5}L·mol^{-1}·s^{-1}. The results show that the established kinetic model aligns well with experimental data.

CRediT authorship contribution statement

Hui Yang: Writing – review & editing, Writing – original draft, Methodology, Investigation, Formal analysis, Data curation, Conceptualization. **Daofan Ma:** Writing – review & editing, Writing – original draft, Validation, Supervision, Methodology, Investigation, Funding acquisition, Conceptualization. **Chunying Zhu:** Writing – review & editing, Methodology, Investigation. **Taotao Fu:** Writing – original draft, Methodology, Investigation. **Guangwei Wang:** Conceptualization, Methodology, Supervision, Writing – review & editing. **Youguang Ma:** Writing – review & editing, Supervision, Resources, Project administration, Funding acquisition, Conceptualization.

Declaration of competing interest

The authors declare that they have no known competing financial interests or personal relationships that could have appeared to influence the work reported in this paper.

Acknowledgments

This work is financially supported by the National Natural Science Foundation of China (No. 22308249), China Postdoctoral Science Foundation (No. 2023M732587, 2024T170644), and the Key Project of State Key Laboratory of Chemical Engineering (No. SKL-ChE-23Z03).

Appendix A. Supplementary data

Supplementary data to this article can be found online at https://doi.org/10.1016/j.ces.2025.121791.

Data availability

Data will be made available on request.

References

Afsina, C.M.A., Aneeja, T., Neetha, M., Anilkumar, G., 2021. Copper-catalyzed cross-dehydrogenative coupling reactions. Eur. J. Org. Chem. 2021, 1776–1808.
Barata-Vallejo, S., Cooke, M.V., Postigo, A., 2018. Radical fluoroalkylation reactions. ACS Catal. 8, 7287–7307.
Belhomme, M.C., Besset, T., Poisson, T., Pannecoucke, X., 2015. Recent progress toward the introduction of functionalized difluoromethylated building blocks onto C(sp2) and C(sp) centers. Chem.-A Eur. J. 21, 12836–12865.
Britton, R., Gouverneur, V., Lin, J.-H., Meanwell, M., Ni, C., Pupo, G., Xiao, J.-C., Hu, J., 2021. Contemporary synthetic strategies in organofluorine chemistry. Nat. Rev. Methods Primers 1, 47.
Chen, X.-T., Zhang, L.-L., Zhou, L.-Y., Wang, S.-H., Chen, J.-F., 2024. Mechanism and kinetics study of the chemically initiated oxidative polymerization of hexafluoropropylene. AlChE J. 70, e18534.
Dong, D.Q., Yang, H., Shi, J.L., Si, W.J., Wang, Z.L., Xu, X.M., 2020. Promising reagents for difluoroalkylation. Org. Chem. Front. 7, 2538–2575.
Feng, Z., Min, Q.Q., Zhao, H.Y., Gu, J.W., Zhang, X.G., 2015. A general synthesis of fluoroalkylated alkenes by palladium-catalyzed heck-type reaction of fluoroalkyl bromides. Angew. Chem. Int. Ed. 54, 1270–1274.
Feng, Z., Xiao, Y.L., Zhang, X.G., 2018. Transition-metal (Cu, Pd, Ni)-catalyzed difluoroalkylation via cross-coupling with difluoroalkyl halides. Acc. Chem. Res. 51, 2264–2278.
Ghattas, W., Hess, C.R., Iacazio, G., Hardré, R., Klinman, J.P., Réglier, M., 2006. Pathway for the stereocontrolled Z and E production of α,α-difluorine-substituted phenyl butenoates. J. Org. Chem. 71, 8618–8621.
Huang, H., Li, Y., 2017. Sustainable difluoroalkylation cyclization cascades of 1,8-enynes. J. Org. Chem. 82, 4449–4457.
Jia, T., He, Q., Ruscoe, R.E., Pulis, A.P., Procter, D.J., 2018. Regiodivergent copper catalyzed borocyanation of 1,3-dienes. Angew. Chem. Int. Ed 57, 11305–11309.
Krys, P., Matyjaszewski, K., 2017. Kinetics of atom transfer radical polymerization. Eur. Polym. J. 89, 482–523.
Lai, Y.-L., Lin, D.-Z., Huang, J.-M., 2017. Copper-catalyzed decarboxylative difluoroalkylation and perfluoroalkylation of α,β-unsaturated carboxylic acids. J. Org. Chem. 82, 597–605.
Laru, S., Ghoshal, S., Sarkar, P., Hajra, A., 2024. Unusual regioselective C–H difluoroalkylation of heteroarenes under photoredox catalysis. Org. Lett. 26, 5098–5104.
Lee, T.C., Tong, Y., Fu, W.C., 2023. Advances in continuous flow fluorination reactions. Chem.- Asian J. 18.
Lemos, A., Lemaire, C., Luxen, A., 2019. Progress in difluoroalkylation of organic substrates by visible light photoredox catalysis. Adv. Synth. Catal. 361, 1500–1537.
Li, C., Cao, Y.-X., Wang, R., Wang, Y.-N., Lan, Q., Wang, X.-S., 2018a. Cobalt-catalyzed difluoroalkylation of tertiary aryl ketones for facile synthesis of quaternary alkyl difluorides. Nat. Commun. 9, 4951.
Li, D., Mao, T., Huang, J., Zhu, Q., 2018b. Copper-catalyzed bromodifluoroacetylation of alkenes with ethyl bromodifluoroacetate. J. Org. Chem. 83, 10445–10452.
Li, S., Xiang, X., Wang, Z., Zhu, C., Ma, Y., Fu, T., 2024. Uniformity and stability of droplet formation at T-junctions in symmetrical microchannels. Chem. Eng. J. 481, 148718.
Li, T., Luo, Y.H., Wu, Z.F., Xiao, T.B., Jiang, Y.B., Qin, G.P., 2021. Dual Fe/Pd-catalyzed reductive cross-coupling: constructing gem-difluoroallylenes with alkenyl bromides and bromodifluoromethanes. Eur. J. Org. Chem. 2021, 6700–6704.
Matyjaszewski, K., Tsarevsky, N.V., 2014. Macromolecular engineering by atom transfer radical polymerization. J. Am. Chem. Soc. 136, 6513–6533.
Mu, Y., Fan, J., Chu, B., Zhong, S., Cheng, Y., 2024. Synthesis of N-vinylcarbazole from acetylene by a continuous high-pressure liquid-phase process with inherent safety. Chem. Eng. J. 493, 152642.
Nanda, A.K., Matyjaszewski, K., 2003. Effect of [PMDETA]/[Cu(I)] ratio, monomer, solvent, counterion, ligand, and alkyl bromide on the activation rate constants in atom transfer radical polymerization. Macromolecules 36, 1487–1493.
Pasca, F., Gelato, Y., Andresini, M., Serbetci, D., Natho, P., Romanazzi, G., Degennaro, L., Colella, M., Luisi, R., 2025. Continuous flow decarboxylative monofluoroalkylation enabled by photoredox catalysis. JACS Au 5, 684–692.
Pintauer, T., Matyjaszewski, K., 2008. Atom transfer radical addition and polymerization reactions catalyzed by ppm amounts of copper complexes. Chem. Soc. Rev. 37, 1087–1097.
Rao, M., Wei, Z.W., Yuan, Y.F., Cheng, J.J., 2020. Copper-catalyzed C-H difluoroalkylation of coumarins with fluoroalkyl bromides. ChemCatChem 12, 5256–5260.
Russo, D., Tomaiuolo, G., Andreozzi, R., Guido, S., Lapkin, A.A., Di Somma, I., 2019. Heterogeneous benzaldehyde nitration in batch and continuous flow microreactor. Chem. Eng. J. 377, 120346.
Schwolow, S., Ko, J.Y., Kockmann, N., Röder, T., 2016. Enhanced heat transfer by exothermic reactions in laminar flow capillary reactors. Chem. Eng. Sci. 141, 356–362.
Shi, S., Tian, J., Luo, Y., 2022. Recent advances in fluorinated products biosynthesis. Bioresour. Technol. Rep. 20, 101288.

Song, J., Cui, Y., Sheng, L., Wang, Y., Du, C., Deng, J., Luo, G., 2022. Determination of nitration kinetics of p-Nitrotoluene with a homogeneously continuous microflow. Chem. Eng. Sci. 247, 117041.
Spennacchio, M., Colella, M., Andresini, M., Dibenedetto, R.S., Graziano, E., Aramini, A., Degennaro, L., Luisi, R., 2023. Unlocking geminal fluorohaloalkanes in nucleophilic fluoroalkylation chemistry: generation and trapping of lithiumfluorocarbenoids enabled by flow microreactors. Chem. Commun. 59, 1373–1376.
Tarantino, G., Hammond, C., 2018. Catalytic formation of C(sp^3)-F bonds via heterogeneous photocatalysis. ACS Catal. 8, 10321–10330.
Taylor, M.J.W., Eckenhoff, W.T., Pintauer, T., 2010. Copper-catalyzed atom transfer radical addition (ATRA) and cyclization (ATRC) reactions in the presence of environmentally benign ascorbic acid as a reducing agent. Dalton Trans. 39, 11475–11482.
Wang, Q., Bian, Y., Dhawan, G., Zhang, W., Sorochinsky, A.E., Makarem, A., Soloshonok, V.A., Han, J., 2024. FDA approved fluorine-containing drugs in 2023. Chin. Chem. Lett. 35, 109780.
Wang, X.Y., Zhao, S., Liu, J.S., Zhu, D.S., Guo, M.J., Tang, X.Y., Wang, G.W., 2017. Copper-catalyzed C-H difluoroalkylations and perfluoroalkylations of alkenes and (hetero)arenes. Org. Lett. 19, 4187–4190.
Wu, G., Börger, J., Jacobi von Wangelin, A., 2019. A carbene-extended ATRA reaction. Angew. Chem. Int. Ed. 58, 17241–17245.
Xu, Q., Chen, J., Wang, Z., Zang, Y., Li, G., Zhu, F., Liu, D., Sun, C., 2023. Two-step flow synthesis of Olaparib in microreactor: route design, process development and kinetics research. Chem. Eng. J. 471, 144304.
Yan, Z., Du, C., Wang, Y., Deng, J., Luo, G., 2022a. Dehydrochlorination of β-chlorohydrin in continuous microflow system: reaction kinetics and process intensification. Chem. Eng. J. 444, 136498.
Yan, Z.F., Tian, J.X., Du, C.C., Deng, J., Luo, G.S., 2022b. Reaction kinetics determination based on microfluidic technology. Chin. J. Chem. Eng. 41, 49–72.
Zhang, F., Min, Q.Q., Zhang, X.G., 2015. Palladium-catalyzed heck-type difluoroalkylation of alkenes with functionalized difluoromethyl bromides. Synthesis-Stuttgart 47, 2912–2923.
Zhang, S.K., Weniger, F., Ye, F., Rabeah, J., Ellinger, S., Zaragoza, F., Taeschler, C., Neumann, H., Brückner, A., Beller, M., 2020. Selective nickel-catalyzed fluoroalkylations of olefins. Chem. Commun. 56, 15157–15160.